STUDY OF FUEL BLOCK COLLISION IN HTGR CORE*

F.-K. TZUNG

General Atomic Company,
P.O. Box 81608, San Diego, California 92138, U.S.A.

SUMMARY

Analytical and experimental studies have been performed to determine the effects of the collision of fuel blocks in the HTGR core during seismic events. In this paper, the study of contact phenomena, such as stress wave propagation, contact time and rebound velocity, as well as the numerical method suitable for this study is presented.

The difficulties of treating nonlinear dynamic contact problems have been discussed by many authors. Numerical treatments have been hampered either by the stability of an explicit time integration scheme or the complexity of an implicit scheme. In order to avoid stability problems with the solution scheme, a matrix-vector modification technique, or the Sherman-Morrison method, in conjunction with the finite element method and Newmark's integration scheme is used.

In using finite element methods for structural analysis, the hexagonal graphite block containing fuel holes and coolant holes is idealized by thousands of elements and nodes. The corresponding matrix-vector equation, derived from the variational principle, includes likewise many thousands of components. The decomposition of the matrix for solutions is indeed a time-consuming process, but one which need only be performed once with the method described in this paper. As the surface of the structure comes in contact with another structure, the boundary condition changes are represented by a localized modification to the matrix-vector equation. In considering local plastic deformation, computations are minimized by expressing the relevant modification to the element stiffness matrix in terms of the product of a vector and its transpose. The modification is incorporated into the solution in a manner such that the frequent contact-release phenomenon can be treated with ease.

Convergence of the procedure is demonstrated by solving Hertzian problems. Agreement with Hertz' theorem is obtained with a relatively crude mesh representation and time step size.

Numerical results of corner and flat face impact of similar and dissimilar blocks are presented. A longer contact time and higher peak stress are found as expected for the corner impact. The rebound velocity appears to be lower for blocks with holes than for blocks without holes. Results for a 7-hole block are compared with experiments. The significance of this comparison is discussed.

* Sponsored in part by the U.S. Energy Research and Development Administration under Contract E(04-3)-167, Project Agreement 51.

1. Introduction

In analyzing the response of loosely stacked hexagonal blocks during a seismic event in the High-Temperature Gas Cooled Reactor (HTGR), a spring-mass-damper model was used to approximate the velocity and the impact configuration of core blocks [1] and a finite element model was used to estimate the dynamic stress, the coefficient of restitution, and the contact time for the impact of two or more blocks. In this paper, the latter approach will be discussed.

Numerical treatment of contact problems by finite element methods involves the modification of the matrix-vector equation corresponding to boundary condition changes as two bodies come in contact. Chan and Tuba [2] use an iteration technique for solutions. Francavilla and Zienkiewicz [3] suggested a simple procedure of obtaining flexibility matrices in terms of contact pressures at possible contact points of two bodies which allows the frictionless contact pressures to be solved as a quasi-linear problem. An iteration procedure associated with one-dimensional wave propagation theory was proposed by Hughes, et. al., [4] for dynamic contact problems. Solutions to problems in which an elastic body collides with a rigid wall were obtained by Tzung [5] using the Shermal-Morrison method in minimizing the the computational effort.

The method used in [5] is extended to the consideration of two or more body impact phenomena as well as local plastic deformations. The discretized equation of motion derived from the finite element approach and Newmark's time integration scheme is given in Section 2. The treatment for contact phenomena and local elastic-plastic deformations is given in Sections 3 and 4. The application of the Sherman-Morrison method to compute the response resulting from the aforementioned nonlinearities is discussed in Section 5. Numerical examples are given in Section 6.

2. Discretized Equations of Motion

For a continuum which consists of infinite particles and has the initial configuration, $\Omega(x_i)$, the position, x_i, of each particle at time, t, can be described by its original position, X_i, and displacement, u_i,

$$x_i(t) = X_i + u_i(t), \quad i = 1, 2, 3. \tag{1}$$

The linearized equation of motion derived from the finite element approximation [6] for the continuum can be written as

$$[M]\{\ddot{u}\} + [K]\{u\} = \{R\}, \tag{2}$$

where [M], the mass matrix, $\{\ddot{u}\}$ and {u} are the acceleration and displacement vectors; [R], the load vector; [K], the stiffness matrix which is obtained by the assembly of all element stiffness matrices, $[K]_n$, defined in sub-regions, Ω_n,

$$[K]_n = \int_{\Omega_n} [B]^T [C] [B] \, dV \tag{3}$$

[B] is the linear strain-displacement transformation matrix; [C] is the material property matrix. The linearized equations restrict the method to small strain and rotation problems.

This restriction can be removed by placing a term corresponding to the difference between the small and the large deformation theories on the right-hand side [6].

Equation (2) can be solved by either an implicit or an explicit time integration scheme. In considering the nonlinear dynamic contact problem, an unconditionally stable implicit scheme appears to be desirable [7]. As an example, the integration method of Newmark is used, i.e.,

$$\Delta\dot{u} = (\ddot{u} + \frac{1}{2}\Delta\ddot{u})\,\Delta t, \text{ and } \Delta u = (\dot{u} + \frac{1}{2}\Delta\dot{u})\,\Delta t \tag{4}$$

where $u = u(t)$; $\Delta u = u(t + \Delta t) - u(t)$; $\dot{u}$, the velocity; $\ddot{u}$, the acceleration. Consequently, we obtain an incremental relation from equation (2),

$$[A]\,\{\Delta u\} = \{b\} \tag{5}$$

where $[A] = \frac{4}{(\Delta t)^2}\,[M] + [K]$,

$$\{b\} = \{R(t + \Delta t) - R(t)\} + [M]\,\{\frac{4\dot{u}}{\Delta t} + 2\,\ddot{u}\}$$

3. Treatment for Contact Phenomena

Since the above formulation remains the same when two disconnected continua are considered, we shall regard eq. (5) as a valid matrix-vector equation in approximating the motion of two or more disconnected solids. The equation must be modified when the two solids come in contact. At two typical points in contact, the normal surface tractions, R^p of one solid and R^q of another solid, and the corresponding normal velocity components v^p and v^q, satisfy the relations, $R^p + R^q = 0$ and $v^p = v^q$. If the surface normal does not coincide with one of the coordinate axes, a local coordinate transformation or the pre-and the post-multiplication of an orthogonal coordinate transformation matrix to the [A] matrix may be made such that the relation between the normal components of the traction and the velocity can be incorporated into eq. (5). Assuming the pth and the qth equations describe the relation between kinematic variables and the surface tractions, R^p and R^q, the required modifications to approximate the contact phenomenon can be expressed in the following form:

$$([A] + [\{I._p\}\,\{A_q.\}] - [\{I._q\}\{A_q. - I_q. + I_p.\}])\{\Delta u\} = \{b\} - \{I._p\}(R^p + R^q - b^q) - \{I._q\}b^q \tag{6}$$

The dot notation used is that of Bodewig [8]. Thus $\{A_i.\}$ is the i-th row of the matrix [A], $\{A._i\}$ its i-th column. [I] is the identity matrix. The 2nd term on both left and right of the above equality assumes the relation $R^p + R^q = 0$ in the p-th equation of (6); the 3rd term replaces the q-th equation by $\Delta u^p = \Delta u^q$. Similar treatment can be made to take care of the friction effect of two bodies in contact by imposing a relation between the tangenital surface tractions. The advantage of writing the modifications in the form of the product of a vector with the transpose of another vector will be seen in Section 5.

4. Treatment for Local Elastic-Plastic Deformations

In considering elastic-plastic deformation, an incremental stress-strain relation is assumed:

$$d\sigma_{ij} = C_{ijkl}\, de_{kl} \qquad i,j,k,l = 1,2,3 \tag{7}$$

where $d\sigma_{ij}$ and de_{ij} are the incremental stress and strain tensors, respectively; the summation convention of tensor calculus for the lower indices of a variable is adopted. The coefficients C_{ijkl} satisfies the following relation:

$$C_{ijkl} = C_{klij} = C_{ijlk} = C_{jikl}$$

and can be written as

$$C_{ijkl} = C^E_{ijkl} - C^P_{ijkl} \quad . \tag{8}$$

C^E_{ijkl} is the elastic modulus and C^P_{ijkl} is a function of current stresses, σ_{ij}, and other state variables such as plastic strain, e^P_{ij} and hardening parameter, k. In considering infinitesimal deformation, one may write the elastic strain increment as the difference between the total strain and the plastic strain increments; hence,

$$d\sigma_{ij} = C^E_{ijkl}\,(de_{ij} - de^P_{ij}) \quad . \tag{9}$$

To define C^P_{ijkl}, a yield criterion

$$f(\sigma_{ij}, e^P_{ij}, k) = 0 \tag{10}$$

and the flow rule

$$de^P_{ij} = \frac{\partial f}{\partial \sigma_{ij}}\, d\eta \tag{11}$$

are used [9]. Using Eqs. (9) and (11) and the condition that f = 0 must always be satisfied during a continuous plastic flow, i.e.,

$$\frac{\partial f}{\partial \sigma_{ij}}\, d\sigma_{ij} + \frac{\partial f}{\partial e^P_{ij}}\, de^P_{ij} + \frac{\partial f}{\partial k}\, dk = 0 \quad , \tag{12}$$

the scalar $d\eta$ is obtained:

$$d\eta = C^E_{ijkl}\, \frac{\partial f}{\partial \sigma_{kl}}\, de_{ij}/h^2 \quad ,$$

$$\text{where} \quad h^2 = \frac{\partial f}{\partial \sigma_{ij}}\, C^E_{ijkl}\, \frac{\partial f}{\partial \sigma_{kl}} - \frac{\partial f}{\partial e^P_{ij}}\, \frac{\partial f}{\partial \sigma_{ij}} - \frac{\partial f}{\partial k}\, \frac{\partial k}{\partial \eta} \tag{13}$$

Substituting Eqs. (11) and (13) into Eq. (9), the stress and total strain relation is obtained;

$$d\sigma_{ij} = C^E_{ijkl} \left(de_{kl} - \frac{\partial f}{\partial \sigma_{kl}} C^E_{mnpq} \frac{\partial f}{\partial \sigma_{pq}} \frac{de_{mn}}{h} \right) . \tag{14}$$

From Eqs. (7), (8) and (14),

$$C^P_{ijkl} = h^{-2} C^E_{ijmn} \frac{\partial f}{\partial \sigma_{mn}} C^E_{klpq} \frac{\partial f}{\partial \sigma_{pq}} . \tag{15}$$

In considering the symmetry of the stress tensor, the stress-strain relation can be reduced and expressed in terms of six-component stress and strain vector relations, i.e.,

$$d\{\sigma\} = [E - P]\, d\{e\} , \tag{16}$$

where $\{\sigma\} = \{\sigma_{11}, \sigma_{22}, \sigma_{33}, \sigma_{23}, \sigma_{31}, \sigma_{12}\}$; $\{e\} = \{e_{11}, e_{22}, e_{33}, \ldots\}$; and [E] and [P] are the 6x6 elastic modulus and modification matrices related to C^E_{ijkl} and C^P_{ijkl}, respectively. In view of Eq. (16), the matrix [P] is expressible as the product of two vectors,

$$[P] = \{w\}\, \{w\}^T , \tag{17}$$

where $\{w\} = \{w_{11}, w_{22}, \ldots.\}$, and $w_{ij} = h^{-1} C^E_{ijkl} \frac{\partial f}{\partial \sigma_{kl}}$.

As an example, we consider linear isotropic elastic materials, i.e.

$$C^E_{ijke} = \lambda\, \delta_{ij}\, \delta_{k\ell} + 2\mu\, \delta_{ik}\, \delta_{j\ell} , \tag{18}$$

and Prager's kinematic hardening rule [9]

$$f \equiv (\sigma'_{ij} - ce^P_{ij})\, (\sigma'_{ij} - ce^P_{ij}) - k^2 = 0 , \tag{19}$$

where $\sigma'_{ij} = \sigma_{ij} - \frac{1}{3} \sigma_{kk}\, \delta_{ij}$; λ and μ are the Lamé constants; c is the hardening coefficient. Equation (17) can be reduced to

$$w_{ij} = \frac{2\mu(\sigma'_{ij} - ce^P_{ij})}{k\sqrt{2(2\mu + c)}} . \tag{20}$$

Replacing the matrix [C] in equation (3) by [E-P], we obtain

$$[K]_n = \int_{\Omega_n} [B]^T [E] [B]\, dV - \{p\}_n \{p\}^T_n \tag{21}$$

where $\{p\}_n \{p\}^T_n = \int_{\Omega_n} [B]^T \{w\} \{w\}^T [B]\, dV$.

It is clear that eq. (5) can be used to treat plastic deformation by modifying the matrix [A] with the products of a vector and its transpose.

5. Sherman-Morrison Method

As it has been shown that the discretized equation of motion including contact phenomena and plastic behavior can be written in the form

$$[A - \sum_{i=1}^{m} \{p\}_i \{q\}_i^T] \{\Delta u\} = \{f\} . \tag{22}$$

Assuming the solution of eq. (5) is obtained by Choleski's decomposition scheme [10], and the lower and upper triangular matrices, [L] and $[L]^T$, are obtained for the symmetric matrix [A], i.e.

$$[A] = [L] [L]^T , \tag{23}$$

the solution to eq. (22) is readily obtainable by the modified Sherman-Morrison method [11] as

$$\{\Delta u\} = [L]^{T^{-1}} \left(\{f^*\} + \sum_{i=1}^{m} \{p^*\}_i y_i\right) \tag{24}$$

where y_i is the solution of

$$\sum_{i=1}^{m} B_{ij} y_i = C_j \quad , \quad j = 1,m$$

and the other terms are defined as $\{p^*\}_i = [L]^{-1} \{p\}_i$, $\{q^*\}_i = [L]^{-1} \{q\}_i$, $\{f^*\} = [L]^{-1} \{f\}$, $B_{ij} = \delta_{ij} - \{q^*\}_j^T \{p^*\}_i$, $C_j = \{q^*\}_j^T \{f^*\}$, $\delta_{ij} = 1$ for $i = j$, and $=0$ for $i \neq j$. The notations, $[L]^{-1}$ and $[L]^{T^{-1}}$, are referred to as the forward elimination and the backward substitution process respectively.

In applying eq. (24) to solve eq. (6), we observe that $\{L^{-1}A._q\}^T \{L^{-1}I._p\} = \delta_{pq}$, and $\{I_p. - I_q.\} \{\Delta u\} = \Delta u^p - \Delta u^q = 0$. Thus the multiplication of $\{I_p. - I_q.\} [L]^{T^{-1}} [L]^{-1}$ on both sides of eq. (6) provides one equation for the unknown $\{A_q.\} \{\Delta u\}$. The coefficient for the unknown is equal to the value of $\{I_p. - I_q.\} [L]^{T^{-1}} [L]^{-1} \{I._p - I._q\}$. Because of the symmetry, the value for the coefficient can be obtained by applying the forward elimination process to the vector $\{I._p - I._q\}$ and calculating the inner product of the resulting vector by itself. In applying eq. (24) to solve eq. (21), we can minimize computation by performing $\{p^*\}_i = \{q^*\}_i = [L]^{-1} \{p\}_i$. Becasue of that we have deliberately made $\{p\}_i = \{q\}_i$ in eq. (21). The advantage of this process is the ease of incorporating modifications into solutions. Once the triangular matrix [L] and the vectors $\{p^*\}_i$ and/or $\{q^*\}_i$ have been computed, the frequent changes in conditions (contact-and-release, yield-and-not-yield) can be treated by either incorporating or not-incorporating the modifications into the solution.

6. Results and Discussions

Spheres with density $\rho = 1760$ kg/m^3, Young's modulus E = 6.2 GPa and Poisson's ratio 0.125, were idealized by 30 axisymmetrically isoparametric elements and 40 nodes. The contact times were .41 msec and .69 msec for 50.8 mm and 88.9 mm diameter spheres, respectively.

This result appears in excellent agreement with Hertz's theory [12]. In Hertz's theory, he proposed to regard the strain produced in each sphere by impact as a local static effect produced gradually and subsiding gradually. The agreement indicates the participation of higher frequency modes in the solution is not important. Indeed, no significant differences have been found in solutions obtained by different time step sizes for this problem.

Flat face as well as corner collisions of solid hexagonal blocks were analyzed through the idealization of the hexagon into 324 isoparametric plane stress elements and 361 nodes. The stress waves generated by the flat face collision of two identical blocks are plotted in Fig. 1. It appears that the response at the center of the block can be fairly well approximated by plane wave theory, i.e., the stress amplitude and the pulse duration can be approximated by $\rho v C_d$ and $2\ell/C_d$ respectively, where ρ is the density, v the initial velocity of the block, C_d the dilatational wave speed, and ℓ the characteristic length of the hexagon. The shear wave speed is indicated as C_s in Fig. 1. The stress amplitude at the corner, however, reaches 4.1 $\rho v C_d$. The response for a corner collision is given in Figs. 2 and 3. The stress amplitude at corner A reaches 7.2 $\rho v C_d$ while the stress amplitude at corner B reduces to 0.7 $\rho v C_d$. Significant differences in wave forms at the center, D, of the block can be seen by comparing Figs. 1 and 3.

The 1/5th scale test block which contains 7 holes in a hexagon was idealized as shown in Fig. 4. Because a flat face collision was analyzed, the half-block model was used with the assumption of zero normal displacement components on the axis of symmetry. Displacements at the center of the contact surface during the collision were plotted in Fig. 5. The total contact time is approximately equal to 0.25 msec while the plane wave requires only 0.085 msec to travel from the contact surface to the opposite face and back. As a result, there are several intervals of contact and release as can be seen in Fig. 5. Hoop stresses at points 31 and 176 (see Fig. 4) are plotted in Fig. 6. High-frequency waves were observed at point 31. The time differences between two subsequent peaks are approximately equal to $2\ell_1/C_d$, where ℓ_1 is defined in Fig. 4.

At an impact velocity of 0.5 m/sec, the rebound velocities for flat face collision are approximately equal to 0.45 m/sec for solid blocks and 0.38 m/sec for blocks with 7 holes. The geometric dispersion of waves in a complex structure appears to reduce the block rebound velocity substantially. The rebound velocity for the corner collision of solid blocks is 0.34 m/sec which provides a measure of the importance of impact configurations.

The measured contact time for the flat face collision of the 1/5th scale blocks is 0.4 m/sec. Since a perfect flat face collision of elastic bodies has been assumed, the contact time obtained by analyses appears to be shorter than that obtained by experiments. Nevertheless, an efficient numerical method has been developed and continuing efforts will be made analytically as well as experimentally to better understand this non-linear dynamic contact behavior.

References

[1] LEE, T. H., WESLEY, D. A., "Nonlinear Seismic Response of a Series of Interacting Fuel Columns Consisting of Stacked Elements," 3rd Int'l. Conf. on Structural Mechanics in Reactor Technology, K8/5, London, 1975.

[2] CHAN, S. K., TUBA, I. S., "A Finite Element Method for Contact Problems of Solid Bodies --Part I. Theory and Validation," Int. J. Mech. Sci. 13, 615-625 (1971).

[3] FRANCAVILLA, A., ZIENKIEWICZ, O. C., "A Note on Numerical Computation of Elastic Contact Problems," Intl. J. for Numerical Method in Engineering, 9, 913-924 (1975).

[4] HUGHES, T. J. R., TAYLOR, R. L., CURNIER, A., KANOKNUKULCHAI, W., "Finite Element Formulation and Solution of a Class of Contact-Impact Problems in Continuum Mechanics," 3rd Int'l. Conf. on Structural Mechanics in Reactor Technology, J5/5, London, 1975.

[5] TZUNG, F., ."Fuel Block Collision Study by a Numerical Integration Method," General Atomic Report, GA-A13431, May 1975.

[6] BATHE, K. L., WILSON, E. L., IDING, R. H., "NONSAP, A Structural Analysis Program for Static and Dynamic Response of Nonlinear Systems," SESM Report No. 74-3, Dept. of Civil Engineering, Univ. of California, Berkeley, February 1974.

[7] BATHE, K. L., WILSON, E. L., "Stability and Accuracy Analysis of Direct Integration Methods," Earthquake Engineering and Structural Dynamics, 1, 283-291 (1973).

[8] BODEWIG, E., "Matrix Calculus", 2nd Edn., North Holland Publ. Co., Amsterdam, 1959.

[9] PRAGER, W., "Theory of Plasticity: A Survey of Recent Achievements," Proc. Inst. Mech. Engrs. 169, 41-57, (1955).

[10] RALSTON, A., "A First Course in Numerical Analysis," McGraw-Hill Book Company, New York, 1956.

[11] KAVLIE, D., GRAHAM, H., POWER, J., "Efficient Reanalysis of Modified Structures," J. of Structural Division, Am. Soc. Civil Eng. 96, 377-392 (1971).

[12] LOVE, A. G., "A Treatise on the Mathematical Theory of Elasticity," Dover Publication, New York, 1944.

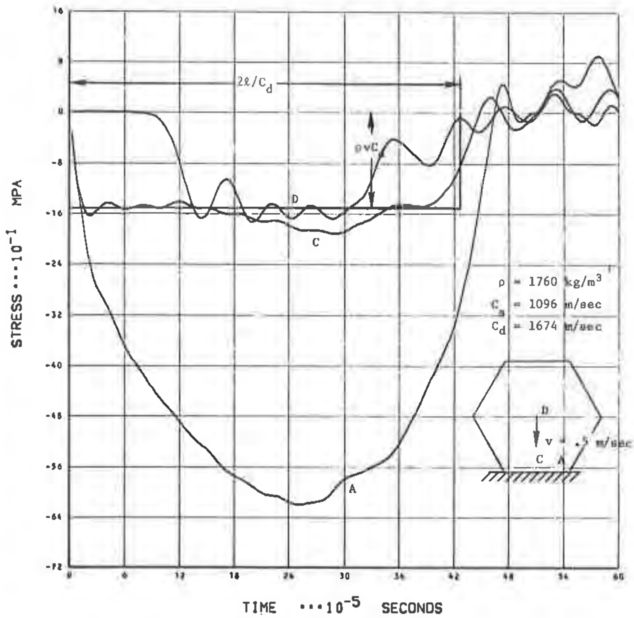

Fig. 1 Stress Waves Generated by Flat Face Collisions.

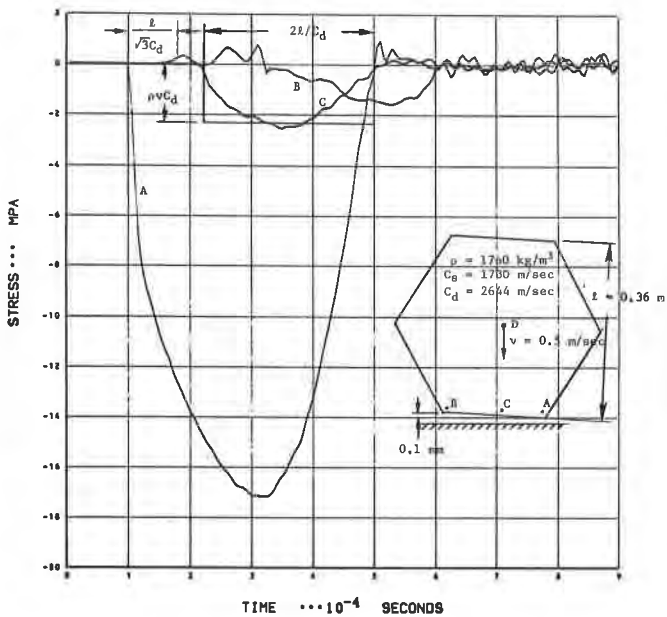

Fig. 2 Stress Waves at the Contact Surface Generated by Corner Collision.

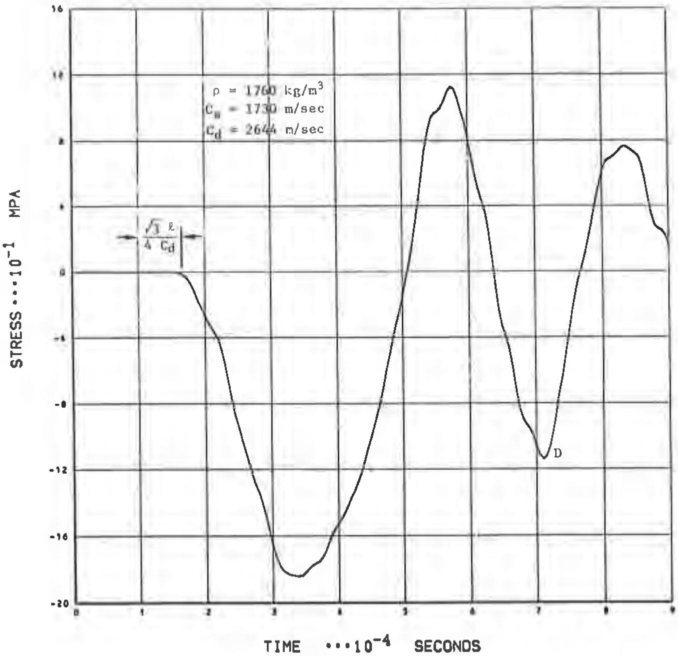

Fig. 3 Stress Waves at the Center of the Block Generated by a Corner Collision.

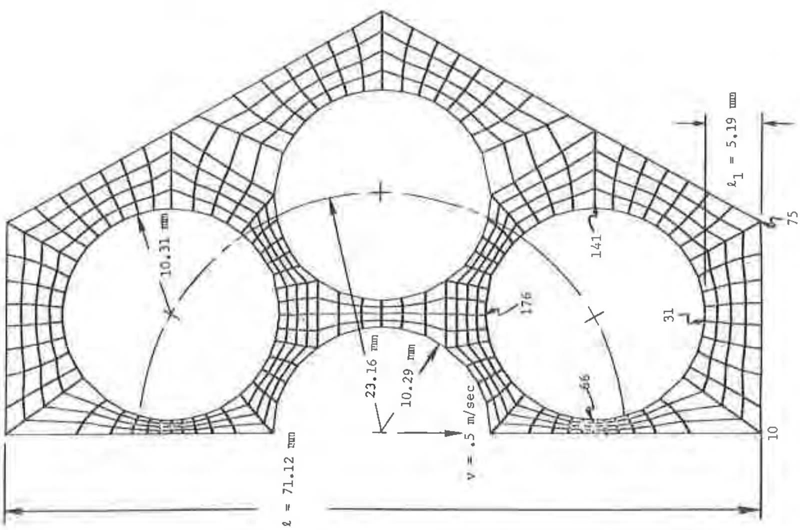

Fig. 4 Finite Element Idealization of the 1/5th Scale Test Block.

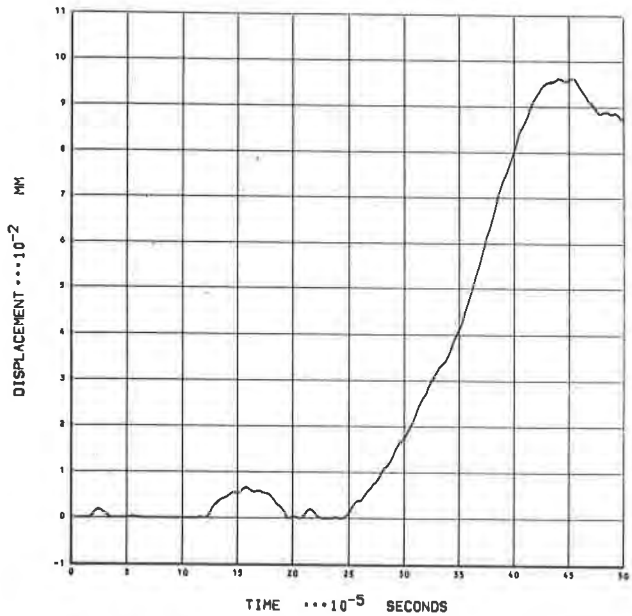

Fig. 5 Displacements at the Center of the Contact Surface during the Flat Face Collision of the 1/5th Scale Test Block.

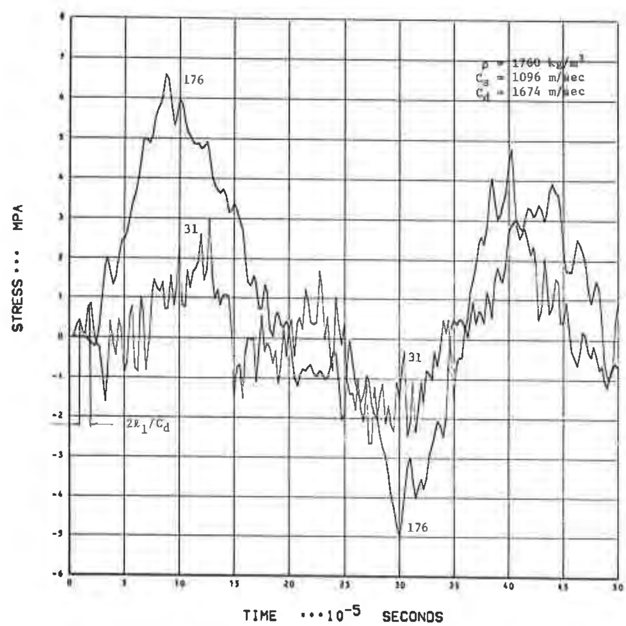

Fig. 6 Hoop Stresses at Points 31 and 176 for the Flat Face Collision of the 1/5th Scale Test Block.